Viscoelastic Properties and Phase Behavior of 12-*tert*-Butyl Ester Dendrimer/Poly(methyl methacrylate) Blends

S. K. EMRAN,[1] Y. LIU,[1] G. R. NEWKOME,[2] J. P. HARMON[1]

[1]Department of Chemistry, University of South Florida, Tampa, Florida 33620

[2]Department of Polymer Science, University of Akron, Akron, Ohio 43325

Received 5 May 2000; revised 28 March 2001; accepted 9 April 2001

ABSTRACT: This study used refractometry, ultraviolet–visible spectroscopy, Fourier transform infrared spectroscopy, differential scanning calorimetry, and dielectric analysis to assess the viscoelastic properties and phase behavior of blends containing 0–20% (w/w) 12-*tert*-butyl ester dendrimer in poly(methyl methacrylate) (PMMA). Dendritic blends were miscible up through 12%, exhibiting an intermediate glass-transition temperature (T_g; α) between those of the two pure components. Interactions of PMMA C═O groups and dendrimer N—H groups contributed to miscibility. T_g decreased with increasing dendrimer content before phase separation. The dendrimer exhibited phase separation at 15%, as revealed by Rayleigh scattering in ultraviolet–visible spectra and the emergence of a second T_g in dielectric studies. Before phase separation, clear, secondary β relaxations for PMMA were observed at low frequencies via dielectric analysis. Apparent activation energies were obtained through Arrhenius characterization. A merged $\alpha\beta$ process for PMMA occurred at higher frequencies and temperatures in the blends. Dielectric data for the phase-separated dendrimer relaxation (α_D) in the 20% blend conformed to Williams–Landel–Ferry behavior, which allowed the calculation of the apparent activation energy. The α_D relaxation data, analyzed both before and after treatment with the electric modulus, compared well with neat dendrimer data, which confirmed that this relaxation was due to an isolated dendrimer phase. © 2001 John Wiley & Sons, Inc. J Polym Sci Part B: Polym Phys 39: 1381–1393, 2001

Keywords: dendrimer; blends; miscibility; phase separation; dielectric analysis

INTRODUCTION

Dendrimers[1–7] and hyperbranched[8–11] macromolecules gained interest when Newkome et al.[12] and Tomalia et al.[13] initially reported on dendritic synthesis in the mid 1980s. Studies on the development of new synthetic methods and their physical characterization have since followed. Dendrimers are unique in that their supramolecular properties[14–18] can be carefully controlled, through the manipulation of size, shape, molecular weight, surface chemistry, and topology, to produce well-defined, highly branched architectures.

Recent studies have focused on blends of dendrimers and hyperbranched structures with linear polymers[19,20] because of the promising possibilities of coupling the unique dendritic qualities with the potential of blends to optimize physical, optical, and processing properties for specified uses. Kim and Webster[21] reported lower melt viscosity and improved thermal stability of polystyrene (PS) with the addition of hyperbranched polyphenylenes. Connolly et al.[22] investigated the effect of blending aryl ester dendrimers with bisphenol A polycarbonate (PC), resulting in an increase in free volume with increasing dendrimer

Correspondence to: J. P. Harmon (E-mail: harmon@chuma.cas.usf.edu)

Journal of Polymer Science: Part B: Polymer Physics, Vol. 39, 1381–1393 (2001)

content. Massa et al.[23] reported increased tensile and compressive moduli and decreased strain to break and toughness in aromatic hyperbranched polyester/bisphenol A PC blends with respect to pure PC. Studies were conducted by Carr et al.[24] on 5, 10, and 20% miscible blends of two aryl ester dendrimers with poly(ethylene terephthalate) (PET); the smaller dendrimer acted as a plasticizer in that it reduced PET chain interactions, resulting in a slight decrease in the glass-transition temperature (T_g) with increased dendrimer content. It was also reported to have enhanced molecular orientation for a given draw ratio, which is valuable for oriented PET fiber and film production. The larger, highly branched dendrimer acted as an antiplasticizer; it increased chain entanglement density caused by dendrimer–chain interaction and resulted in a slight increase in T_g with increased dendrimer content. This antiplasticizing effect decreased with the incorporation of smaller, less structurally complex dendrimers. Studies conducted by Bauer and coworkers[25,26] used small-angle scattering and transmission electron microscopy to explore miscible blends of either poly(amido amine) (PAMAM) or poly(propylene amine) (PPI) in a copolymer of methyl methacrylate with 1% methacrylic acid. They also studied ternary blends of 0–10% hydrophobically modified PPI-C_8 dendrimer in the polymer blend PS/poly(vinyl methyl ether) (PVME); an increase in the dendrimer content improved miscibility when the PVME content was high. In addition, they examined interpenetrating polymer networks of 1–25% PAMAM dendrimer polymerized in poly(2-hydroxyethyl methacrylate). They reported a uniform distribution of dendrimers in the matrix, which lacked the signs of clustering encountered with linear polymers. Studies on the use of hyperbranched polyesters as processing aids for linear low-density polyethylene were conducted. Blends of up to 10% hyperbranched polyesters were found to reduce melt viscosities and eliminate surface defects, melt fracture, and sharkskin.[27]

These studies show that the blending of hyperbranched structures and dendrimers with linear polymers is a promising route to novel materials used in modern materials technology. Blends fabricated with dendrimers are of particular interest because these regularly branched, monomolecular structures are prepared in small batches. Blending linear polymers with low concentrations of dendrimers may enhance the physical properties of the linear polymers. Blending, for example, might optimize melt viscosities of linear polymers used in drawing polymeric optical fibers. This application requires strong interactions between the linear polymer and branched structure because any scattering due to phase separation impedes light harvesting in the sample. Conversely, systems with limited interactions are ideal candidates for the fabrication of nanoporous films. Low concentrations of spherical dendrimers dispersed in a system with limited interactions could be removed from a polymer substrate via solvents that selectively dissolve only the dendrimer, leaving nanopores in its place.

The purpose of this study is to characterize the phase behavior in a series of 12-*tert*-butyl ester dendrimer/poly(methyl methacrylate) (PMMA) blends. The *tert*-butyl end groups eliminate strong interactions between end groups and hydrogen-bonding sites on the linear PMMA. However, amide groups within the dendrons are expected to interact with carbonyl groups in the linear polymer. The overall objective is to characterize relaxation behavior, phase behavior, and structure–property relationships. Also of importance is comparing dendrimer blend behavior to that observed in linear polymers blends and in blends of hyperbranched polymers with linear polymers.

The physical characterization of the dendrimer (Fig. 1) used in this work has been previously reported;[28] matrix-assisted laser desorption/ionization time-of-flight mass spectrometry data has revealed that the dendrimer is monomolecular, possessing a single composition. Studies encompassing refractometry, ultraviolet–visible (UV–vis) spectroscopy, Fourier transform infrared (FTIR) spectroscopy, and differential scanning calorimetry (DSC) are herein reported, along with the dielectric analysis (DEA) of primary (α) and secondary (β) relaxations.

EXPERIMENTAL

Materials

The 12-*tert*-butyl ester dendrimer [number-average molecular weight = weight-average molecular weight = 2046; Fig. 1(a)] was synthesized by Dr. Claus Weis of the Center for Molecular Design and Recognition.[29] PMMA [Fig. 1(b)] was manufactured by I.C.I. Acrylics and UV-stabilized with trace amounts of Tinuvin® P. Dendritic blends consisting of 0, 3, 6, 9, 12, 15, 17, and 20% (w/w) 12-*tert*-butyl ester dendrimer/PMMA were formed by the dissolution of the appropriate weight percentage of each

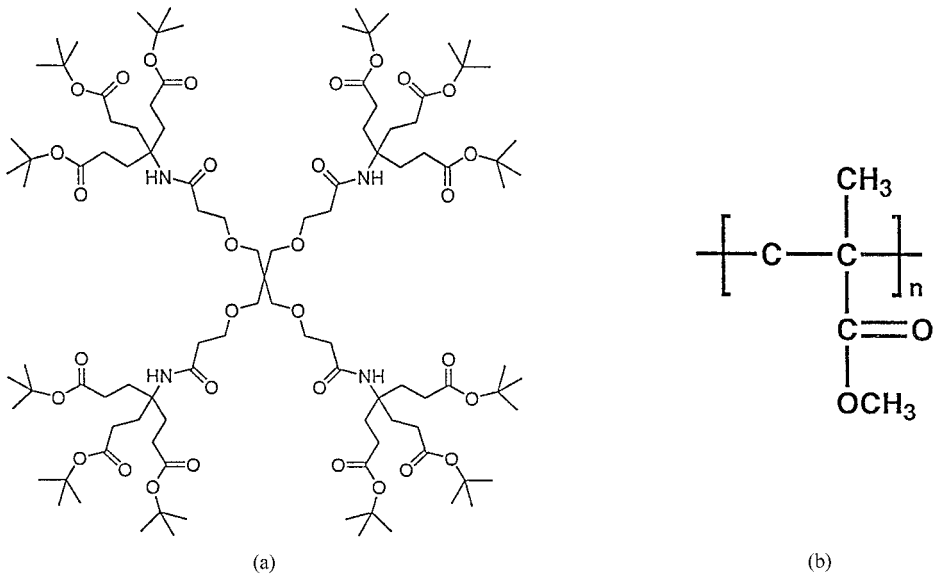

Figure 1. Molecular structures of (a) 12-*tert*-butyl ester dendrimer and (b) PMMA.

component in CH_2Cl_2. Methylene chloride was filtered with a 0.2-μm Teflon Nalgene syringe filter, as were all of the solvents used in this study. Solutions were allowed to slowly evaporate, resulting in the formation of films. These were placed in a vacuum oven at 105 °C for 48 h to remove residual solvent. Blends used for UV–vis spectroscopy and DEA were heat/compression-molded into discs at 175 °C with a Carver Laboratory Hot Press model C and stainless steel molds 0.81 ± 0.01 mm thick and 24.30 ± 0.10 mm in their inner diameter. Samples were allowed to cool slowly to 25 °C before removal from the press.

Methods

Viscosity-Average Molecular Weight (M_v)

M_v of PMMA was determined via the method previously described[30] with the Mark–Houwink–Sakarada parameters: $K = 7.5 \times 10^{-5}$ and $a = 0.70$. M_v was determined to be 107,000.

Refractometry

Refractive indices of 12-*tert*-butyl ester dendrimer and PMMA were determined with an Olympus polarized microscope and a series of refractive-index oil standards obtained from R. P. Cargille Laboratories, Inc. A minute amount of a powdered sample was placed on a glass slide, and a drop of oil was then placed on the sample. The sample–oil boundary was examined at 400× magnification for observation of the Becké line. The appearance of the Becké line, when the microscope was brought into and out of focus, indicated a difference in the refractive indices of the sample and refractive-index oil standard. The refractive index of the sample was obtained by performing several trials with various oil standards until the Becké line was no longer observed, which indicated a match between the refractive index of the oil standard and the dendrimer[31,32] at 25.40 ± 0.05 °C.

UV–vis Spectroscopy

UV–vis spectroscopy was performed with an HP 8452A diode array spectrophotometer and HP 89531A UV–vis operating software. Absorbance data for neat 12-*tert*-butyl ester dendrimer and neat PMMA were obtained from solutions made with high performance liquid chromatography (HPLC)-grade acetonitrile (MeCN); quartz cuvettes with a 1.000 cm path length were used, and MeCN served as the blank. Transmittance percentage spectra for 0–20% blends were obtained from discs 0.81 ± 0.01 mm thick; air served as the blank.

FTIR Spectroscopy

Powdered samples were placed on a 25 × 4 mm KBr disc obtained from Barnes Analytical, Inc., and a drop of filtered CH_2Cl_2 was placed on the powder to dissolve the sample. The solution was then air-dried to achieve a thin film on the KBr

disc. Data were collected on an ATI Mattson Genesis Series FTIR with Winfirst V.2 software.

DSC

With a TA Instruments Thermal Analyst 2000 computer system equipped with data analysis software interfaced with DSC and DEA, DSC experiments were performed on a TA Instrument DSC 2920. Samples (3–5 mg) were sealed in standard aluminum DSC pans. Under a 25 mL/min helium purge, samples were sequentially heated, cooled (programmed cooling in DSC and DEA experiments to subambient temperatures reaching −150 °C was achieved with a TA Instruments liquid nitrogen cooling accessory), and reheated at a rate of 3 °C/min over a 0–150 °C temperature range. The differential heat flow between the sample and reference (empty pan) was measured as a function of temperature. The thermal history of the samples was erased after the first heating; therefore, the T_g's were obtained from the second heating and were taken as the midpoint (inflection point) of the onset and offset of the transition. The DSC has a sensitivity of 0.2 μW, a calorimetric precision of ±1%, a temperature reproducibility of ±0.05 °C, and a temperature accuracy of ±0.1 °C.[33] ΔC_p values, the differences in specific heat capacities in the glassy and rubbery states, were calculated as described.[33]

DEA

With a TA Instruments Thermal Analyst 2000 computer system equipped with data analysis software interfaced with DSC and DEA, DEA was conducted on a TA Instruments DEA 2970. DEA ceramic parallel plate sensors, consisting of two gold-plated electrodes in parallel, were employed, and sensor calibration was conducted under a nitrogen purge of about 500 mL/min, as were experimental runs. Previously molded blend samples were placed on the lower electrode, which sat on the furnace. The upper electrode was attached to a ram that, when lowered, applied a maximum force of 250 N to achieve a minimum spacing of 0.500 mm. The upper electrode measured the generated current, which was converted to an output voltage and amplified. The lower electrode applied a voltage, which induced an electrical field. Spring-loaded electrical probes, protruding from the ram, made contact with electrical contact pads on the sensor to complete signal circuits. The sample response to the electrical field was measured as a function of temperature and frequency (0.1–100,000 Hz). Blends were initially heated to 200 °C (below the degradation temperature of the dendrimer) to soften the samples to achieve 0.500-mm sample spacing between the parallel plates. Samples were then control-cooled to −150 °C and subsequently heated to 200 °C at a heating rate of 3 °C/min. Cole–Cole data were subsequently obtained by the heating of the samples from −150 to 200 °C in 5 °C increments within the given temperature range with 6-min isothermal measurements at each increment. The isothermal measurements allowed data acquisition over the entire frequency range. Capacitance and conductance were measured as a function of temperature and frequency to give the dielectric constant or permittivity, ϵ' (proportional to capacitance), and the loss factor, ϵ'' (proportional to conductance). Because parallel plate spacing and force applied to the sample were continuously monitored and controlled, accuracy and reproducibility were achieved. DEA offers a dielectric constant sensitivity of 0.01 and an isothermal stability of 0.2 °C.[34]

RESULTS AND DISCUSSION

Refractometry

Refractive indices were experimentally determined and calculated for both the pure dendrimer and PMMA from group contribution methods according to Lorentz and Lorenz.[35] The refractive index (η) obtained for the neat 12-*tert*-butyl ester dendrimer was 1.480 ± 0.005. The calculated value of η for the dendrimer was 1.473. An experimental value of 1.490 ± 0.005 was obtained for PMMA. This compares well with the calculated value, 1.484. The mismatch in refractive indices is responsible for the Rayleigh scattering noted and is discussed in the next section.

UV–vis Spectroscopy

Absorbance spectra were obtained for both pure dendrimer and pure PMMA solutions in MeCN. A peak was revealed in the dendrimer spectrum at 196 nm, whereas absorbance in PMMA arose at 214 nm; these peaks were attributed to absorbance from π–π^* electron transitions of the C═O groups.[36–38] The PMMA spectrum revealed additional peaks at 298 and 338 nm, which are associated with absorbance from Tinuvin® P.

The transmittance percentage of 0–20% blends of dendrimer in PMMA is depicted in Figure 2. At 15% and higher, wavelength-dependent Rayleigh

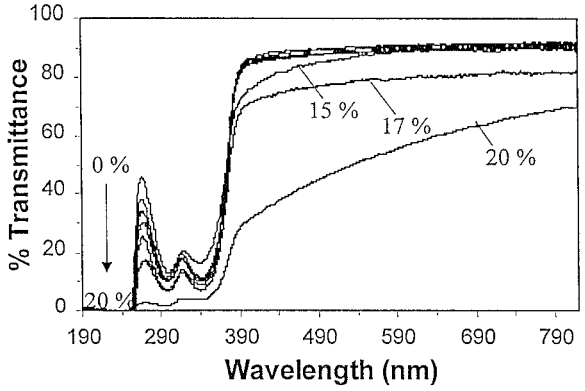

Figure 2. UV–vis spectra for the blends.

scattering was observed.[38–40] This scattering implied phase separation, which arose from a heterogeneous environment consisting of phases with differing refractive indices. UV–vis spectroscopy is a classical method that has been used in miscibility assessments of linear polymer blends.[41] PMMA blends with linear fluorocarbon polymers exhibit Raleigh scattering at the onset of phase separation, as substantiated by other physical measurements.[42,43] This is the first study of which the authors are aware that examines optical-quality, solid samples of dendrimer–linear polymer blends.

FTIR

FTIR measurements were used to assess miscibility by the presence of intermolecular interactions in blends. Hydrogen bonding is the most significant type of molecular interaction that can be observed through IR analysis.[44] The observance of small shifts (<10 cm^{-1}) in linear polymer blends has proven to be a successful method for detecting miscibility.[45] This is achieved by the observation of shifts in the blend peaks arising from various functional groups with respect to those of the pure components, the understanding being that no observable shift implies a lack of interaction.

Several small shifts were exhibited for 0–20% dendritic blends. These included the following: the asymmetrical C—H stretch shifted from 2995 cm^{-1} for 0% blends to 2990 cm^{-1} for 20% blends, the C═O stretch shifted from 1732 to 1730 cm^{-1}, N—H in-plane bending appeared at 1652 cm^{-1} for pure dendrimer and appeared as a shoulder in the higher percentage blends at 1682 cm^{-1}, and the C—N stretch shifted from 1066 to 1068 cm^{-1}. These shifts indicate that hydrogen-bonding interactions of the PMMA side chain (C═O) and amide-containing dendrons (arms) of the dendrimer (N—H) significantly contribute to blend miscibility. FTIR results did show miscibility, however, they gave no information on phase separation.

DSC

T_g's of compatible blends and random copolymers usually decrease with an increasing weight fraction of the component with the lower T_g.[46] T_g of 12-*tert*-butyl ester dendrimer was 40 °C, and that of pure PMMA was 105 °C. Only one intermediate T_g was observed for the blends, including the higher percentage (15–20%) blends, which contained some degree of immiscibility, as observed from UV–vis spectroscopy data. Phase-separated blends are expected to exhibit two T_g's. The experimental results indicate that, for these systems, DSC is not sensitive enough to detect regions of incompatibility in an otherwise miscible blend. Further information on intermolecular effects in blends are obtained by a comparison of the T_g's obtained from experimental methods and those predicted from mathematical expressions such as the Couchman equation:[47]

$$\ln T_g = \frac{K' w_1 \ln T_{g1} + w_2 \ln T_{g2}}{K' w_1 + w_2} \quad k' = \frac{\Delta C_{p1}}{\Delta C_{p2}} \quad (1)$$

where T_g is the glass-transition temperature (K) of the blend, w_1 and w_2 represent the weight fractions of the individual components constituting the binary mixture, and T_{g1} and T_{g2} represent the individual glass-transition temperatures (K) of the two pure components. ΔC_{p1} and ΔC_{p2} represent the difference in specific heat capacities in the glassy and rubbery state. If $\Delta C_p T_g$ is constant and the two T_g's do not differ very much, eq 1 reduces to the Fox equation:[23,48]

$$\frac{1}{T_g} = \frac{w_1}{T_{g1}} + \frac{w_2}{T_{g2}} \quad (2)$$

Values for experimental and predicted T_g's of the blends and pure components are listed in Table I. Values predicted from the Couchman equation are less than those predicted by the Fox equation because of the high value of $\Delta C_{p1}/\Delta C_{p2}$, 2.0. This leads to a weighting of the blend behavior in favor of the dendrimer with the lower T_g. In general, the experimental data supports higher T_g's than those predicted by Couchman's equation, even in

Table I. T_g (°C)

	Dendrimer in Blend (%)	Observed by DSC	Predicted from Couchman Equation	Predicted from Fox Equation
PMMA	0	105	—	—
	3	105	99	103
	6	106	94	100
	9	97	89	98
	12	94	85	96
	15	93	81	94
	17	94	79	92
	20	94	76	90
Dendrimer	100	40	—	—

blends exhibiting no scattering in the optical studies. Couchman[47] pointed out that his derived relation requires miscibility approaching the segmental level. It is tempting to speculate that interactions between the *t*-butyl-capped dendrimer and PMMA do not extend to such a level so that the expected plasticization is limited.[49] Also of interest are observations of these dendrimer blends as they compare to other hyperbranched blends and blends of two linear components. In studies with linear polymers containing strong hydrogen-bonding sites (such as polyamides), hydroxyphenyl-terminated hyperbranched polyesters exhibited blend miscibility similar to that of linear poly(vinyl phenol).[23] This indicates that strong interactions dominate miscibility and mask the architectural effects of the hyperbranches. When the same hydrogen-bonding linear polymers were blended with acetoxy-terminated polyester dendrimers and linear poly(acetoxystyrene) (PAS), miscibility decreased with respect to the hydroxy-terminated systems. However, the hyperbranched structure exhibited higher miscibility than the linear analogue, PAS. It appears as though molecular architecture influences miscibility to a greater extent when hydrogen-bonding interactions are less pronounced. Although both deviations from the Couchman equation and scattering experiments indicate minimal solubility in the dendrimer systems studied herein, conclusions regarding the true nature of architectural influence await further studies with other dendrimer systems.

DEA

DEA experimentation was performed for the further assessment of phase behavior in the blends.[50–53] Spectra obtained from 6-min isothermal measurements in 5 °C increments were used for analysis; this method proved to be more sensitive to the detection of the onset of phase separation than the initial 3 °C/min ramp method. Figure 3 depicts dielectric spectra for neat PMMA and the 12% blend before phase separation from 3 to 3000 Hz; the loss curves shift to higher temperatures with increasing frequencies. The relaxation occurring below T_g at lower frequencies is the β relaxation, which involves rotation of the PMMA ester side group when main-chain motion is frozen. A merged $\alpha\beta$ process, which involves main-chain slippage in PMMA cooperative with side-group rotation, is observed at higher temperatures and frequencies.[50] Dielectric spectra for 15 and 20% blends are shown in Figure 4 after phase separation. Unlike DSC experimentation, DEA allowed the detection of a second T_g arising from the phase-separated dendrimer component (α_D). The initial emergence of the α_D relaxation was observed at 15% and found to be more prominent at higher dendrimer concentrations. This confirmed results from UV–vis spectroscopy data that revealed phase-separated scattering at and above 15%. The increase in conductivity at high temperatures and low frequencies is attributed to increased dendrimer content because significant conductive effects were observed for the neat 12-*tert*-butyl ester dendrimer in a previous study.[28]

As observed from the dielectric spectra (Figs. 3–5), the loss factor (ϵ'') for the PMMA β process decreased in magnitude with increasing dendrimer content up through 15%. This behavior is due to increased PMMA (C═O)–(N—H) dendrimer interactions. As the dendrimer content is increased, more C═O groups interact with N—H groups and, therefore, no longer contribute to the

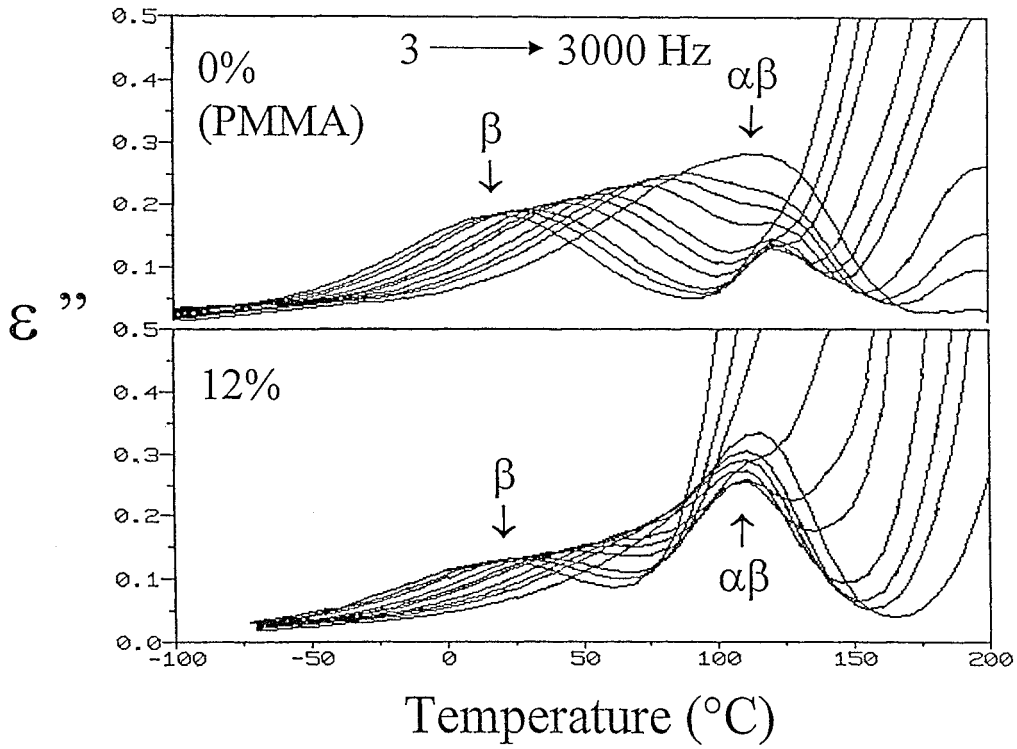

Figure 3. Dielectric spectra before phase separation.

β process. The peak magnitudes for the β relaxation after phase separation (15–20%) remained relatively constant because the dendrimer reached its maximum level of miscibility in PMMA. After phase separation, the β process is attributed to rotation of the noninteracting C═O

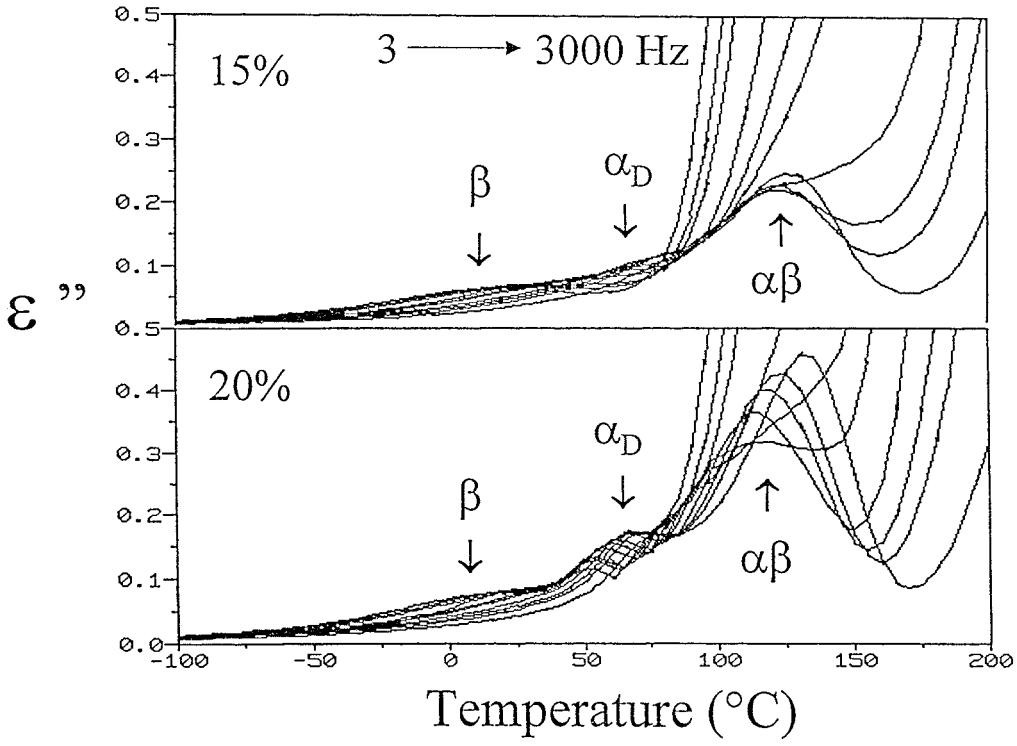

Figure 4. Dielectric spectra after phase separation.

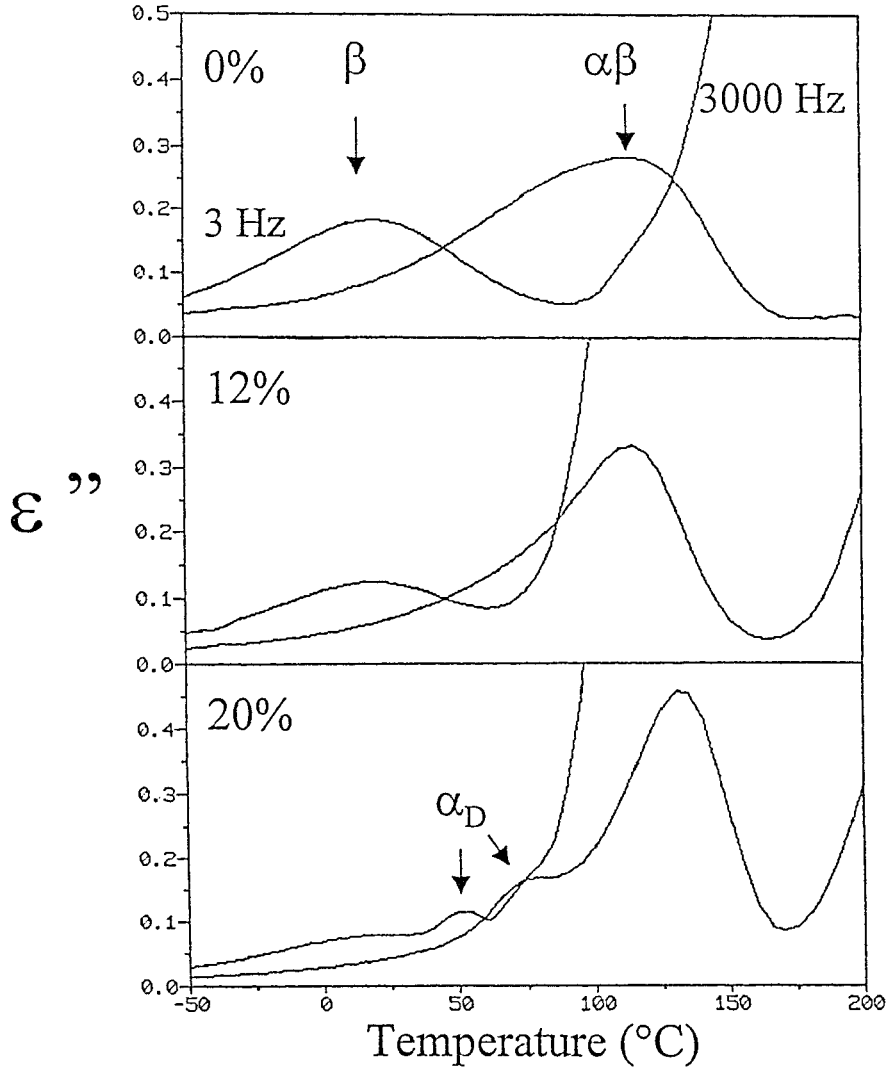

Figure 5. Dielectric spectra at 3 and 3000 Hz.

groups. It can also be observed from Figure 5 that as β diminished, the merging of β with the α process occurred to a lesser extent; the neat PMMA spectrum revealed an $\alpha\beta$ relaxation that was broad compared with that observed for the dendritic blends.

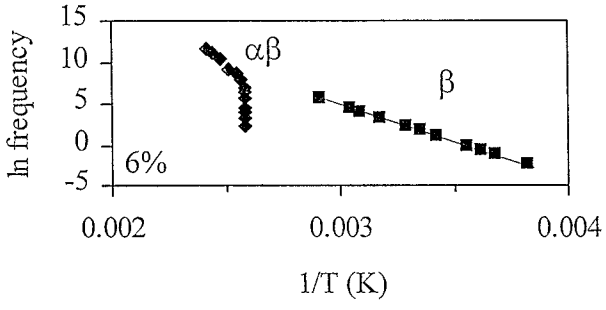

Figure 6. Representative Arrhenius plot before phase separation.

Figure 6 represents a typical plot of ln f_{max} versus $1/T$ (K) observed in the miscible blends. Arrhenius behavior was used to characterize the clear frequency-dependent β relaxations encountered before phase separation.[49] Linear behavior was observed for the pure β process, which was discernible at lower frequencies. Apparent activation energies (ΔH) for the β process were calculated for blends before phase separation (Table II); β relaxations were less prominent after phase separation and could not be characterized. ΔH for PMMA was determined to be 17.6 kcal/mol and is comparable to values found in the literature, 17.4[54] and 19–23 kcal/mol,[49] depending on the frequency range of the data. This value remained constant up through 6% blends; however, a slight

Table II. Arrhenius Apparent Activation Energies

	Dendrimer in Blend (%)	ΔH (kcal/mol) for the β Relaxation
PMMA	0	17.6
	3	17.6
	6	17.6
	9	16.9
	12	16.0
	15	—
	17	—
	20	—
Dendrimer	100	11.8

decrease for 9 and 12% blends was noted. As the dendrimer content increased, the C═O groups from PMMA have increasing interactions with N—H groups. Although ΔH values could not be obtained after phase separation, it is believed that these values should remain relatively constant because, in the dendrimer–PMMA miscible phase, the number of C═O groups available for rotation is constant.

The deviation from linear behavior depicted at higher temperatures in Figure 6 is attributed to motion associated with the $\alpha\beta$ relaxation. This merged process could not be further characterized. Arrhenius plots for PMMA and PMMA/PVDF blends depicting changes in curve behavior between β and $\alpha\beta$ relaxations are also noted in the literature.[54]

Cole–Cole plots (ϵ'' vs ϵ') were constructed for β, α_D, and $\alpha\beta$ processes to evaluate the dielectric strengths.[49,51,55] The dielectric strength, or relaxation strength ($\Delta\epsilon$), was taken as the difference between the low-frequency, relaxed state (ϵ_o) involving contributions from all dipole orientation processes and the high-frequency, unrelaxed state (ϵ_∞), which is void of all dipole orientation contributions due to measurements at high frequencies.[49] Thus, $\Delta\epsilon$ is related to the amount of dipoles per unit volume and the effectiveness of their alignment with the applied electric field. Representative plots for the β and $\alpha\beta$ processes in the blends are shown in Figure 7. Deviation from semicircular behavior indicates a distribution of relaxation times, which is associated with complex molecular motion involving orientation about different axes by rotation.[52,56]

Table III lists $\Delta\epsilon$ values of the β, α_D, and $\alpha\beta$ relaxations. The β-relaxation values for $\Delta\epsilon$ remained fairly constant (0.070 ± 0.002) for all the blends and were smaller in magnitude than those obtained for both the α_D and $\alpha\beta$ processes. Dielectric-strength values for the α_D relaxation obtained for 15, 17, and 20% blends were relatively constant (0.56 ± 0.05), as would be expected because they were derived from the isolated, dendritic environment. For the $\alpha\beta$ process, a decrease in $\Delta\epsilon$ values from 1.43 to 1.01 was observed because the number of dipoles oriented per unit volume decreased. This was caused by the increased dendrimer content, which had a diluting effect due to increased free volume.

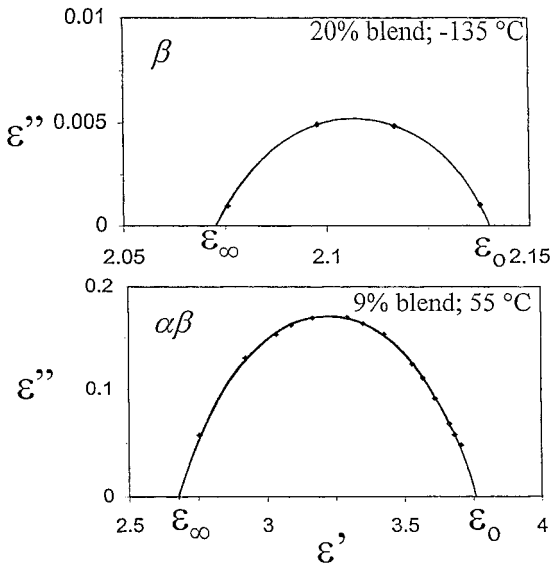

Figure 7. Representative Cole–Cole plots for β and $\alpha\beta$ relaxations.

The dielectric spectrum of the 20% blend, depicted in Figure 4, reveals prominent, frequency-dependent peaks for the highly phase-separated dendrimer (α_D). At each frequency, the peak passes through a maximum at the temperature of the glass relaxation. A plot of the natural log of the frequency versus the inverse temperature at T_g results in a curved behavior that is defined by the Williams–Landel–Ferry (WLF) equation:[28,57,58]

Table III. $\Delta\varepsilon$

	Dendrimer in Blend (%)	β	α_D	$\alpha\beta$
PMMA	0	0.068		1.43
	3	0.068		1.32
	6	0.072		1.24
	9	0.072		1.12
	12	0.069		1.01
	15	0.072	0.51	—
	17	—	0.60	—
	20	0.072	0.56	—

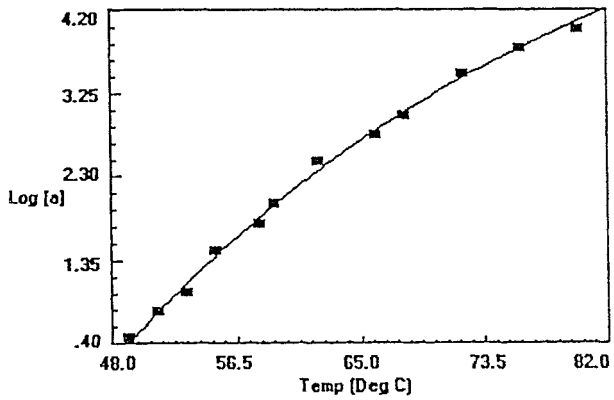

Figure 8. WLF plot for a phase-separated dendrimer (α_D) in a 20% blend after electric modulus treatment.

$$\ln a_T = \frac{-C_1(T - T_0)}{C_2 + (T + T_0)} \quad (3)$$

where a_T is the shift factor that corresponds to frequency; C_1 and C_2 are WLF constants; T is a given temperature; and T_o is the reference temperature, which corresponds to T_g.

Figure 8 depicts a comparable plot of the log of the frequency versus temperature for the dendritic glass transition (α_D) that conforms to WLF behavior. The values for C_1, C_2, and T_o were determined from curve fitting of the data to the WLF equation; these were found to be 9.93, 53.20, and 47 °C, respectively. The universal constants C_1 and C_2 are reported as 17.4 and 51.6,[53,54,58] respectively. ΔH values were subsequently calculated according to the following equation:[59]

$$\Delta H = 2.303\left(\frac{C_1}{C_2}\right)RT_g^2 \quad (4)$$

In a previous study involving the neat 12-*tert*-butyl ester dendrimer,[28] mathematical treatment of the data was required to subtract ionic conductivity effects that obscured the glass transition at high temperatures and low frequencies. To observe the glass transition (α), the data were mathematically treated in terms of the electric modulus,[60] M^*, which is defined as the inverse of complex permittivity, ϵ^*, where $\epsilon^* = \epsilon' - i\epsilon''$ and $M^* = M' + iM''$ such that

$$M' + iM'' = (\varepsilon' - i\varepsilon'')^{-1} \quad (5)$$

$$M' = \frac{\varepsilon'}{(\varepsilon')^2 + (\varepsilon'')^2} \quad \text{and} \quad M'' = \frac{\varepsilon''}{(\varepsilon')^2 + (\varepsilon'')^2} \quad (6)$$

Conductivity effects increased in the dielectric spectra for the dendrimer/PMMA blends with increasing dendrimer content at high temperatures and low frequencies (Figs. 3 and 4). This was expected because data from a previous study[28] revealed the highly conductive nature of the dendrimer. Therefore, to confirm the true nature of the relaxation emerging in the phase-separated blends, the data were further treated to remove conductivity effects. The electric modulus approach was applied to the α_D relaxation (20% blend) before the data were curve-fitted to the WLF equation and ΔH was calculated; this allowed for a better comparison of the neat dendrimer data[28] with the phase-separated dendrimer data (Table IV). WLF data revealed a T_g of 47 °C and C_1 and C_2 constants of 10.50 and 51.80, respectively. These data were in good agreement with WLF data obtained before electric modulus treatment (T_g = 48 °C, C_1 = 9.93, and C_2 = 53.20); this is compared with data previously obtained for the neat dendrimer (T_g = 44 °C, C_1 = 16.5, and C_2 = 76.8).[28] Deviations of phase-separated C_1 and C_2 constants from neat dendrimer data may be due to the limited number of frequencies observed for α_D relaxation in the phase-separated system. The ΔH values were also calculated for the neat dendrimer with electric modulus treatment (99.1 kcal/mol), the phase-separated α_D relaxation in the 20% blend with electric modulus treatment (95.1 kcal/mol), and

Table IV. Dendrimer Data

	Electric Modulus		Without Electric Modulus
α Relaxation	Neat	Phase-Separated 20% Blend	Phase-Separated 20% Blend
T_g (°C), WLF	44	47	48
ΔH (kcal/mol), WLF	99.1	95.1	88.2
ΔM	0.113	0.112	—
$T_{\text{peak max (100 Hz)}}$ (°C)	54	59	62

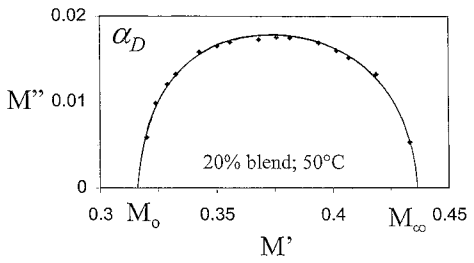

Figure 9. Cole–Cole plot for a phase-separated dendrimer (α_D) in a 20% blend after electric modulus treatment.

the phase-separated α_D relaxation in the 20% blend without electric modulus treatment (88.2 kcal/mol). All of these were in good agreement. Cole–Cole plots have previously been extended to the electric modulus approach, where M'' is plotted as a function of M'.[60] This type of Cole–Cole diagram is depicted in Figure 9 for the complex α_D process in the 20% blend. The dielectric strength (ΔM) was also calculated after treatment with the electric modulus (0.112) and was found to coincide with that of the neat dendrimer (0.113). Table IV also lists the temperatures of the peak maxima at 100 Hz for the α_D relaxation for all three cases; the temperatures are reasonably comparable, although less discrepancy is noted for the electric modulus data. The data shown in Table IV successfully confirm that the α_D process does, in fact, arise from the isolated phase-separated dendrimer component. Therefore, it has been concluded that before phase separation ($\leq$12%), a miscible dendrimer–PMMA phase exists; after phase separation ($\geq$15%), a miscible dendrimer–PMMA phase coexists with an isolated dendrimer phase. The data shown in Table IV were calculated for the 20% blend rather than the 15 and 17% blends because of the more prominent nature of the α_D relaxation in the 20% blend, which allowed for better characterization. This work is significant in that DEA has been proven to serve as a sensitive and effective tool that allows researchers to probe the phase behavior of blends.

No evidence of the Maxwell–Wagner–Sillars (MWS) effect[50,61–64] was observed from DEA on the phase-separated system. The MWS effect arises in a heterogeneous environment when the permittivities and conductivities of the two components cause the accumulation of charges at the phase boundary, which subsequently affects the electric field. Although the conductivity of the blends was found to increase with increasing dendrimer content, this effect was also observed in both the neat dendrimer and the miscible, one-phase dendritic blends. Thus, the inability to characterize conductivity effects arising purely from the MWS effect implies that the two phases are closely associated because of strong interphase interactions. Bánhegyi et al.[65] reported an immiscible blend of 5% polyurethane in polypropylene and determined that mechanical interlocking occurred between phases; interfacial polarization in this heterogeneous system was undetectable. The MWS effect is often, but not always, observed in immiscible blends because its manifestation is dependent on both the material and morphology.[50] A detailed discussion of MWS behavior and equations used to model this interfacial polarization in blends with various morphologies and properties is given in van Beek.[66] Theoretical and experimental discussions on the dielectric spectroscopy of heterogeneous composites are presented by Bánhegyi et al.[65]

CONCLUSION

The miscibility of 12-*tert*-butyl ester dendrimer and PMMA blends is mainly attributed to hydrogen-bonding interactions of the PMMA side chain and amide-containing dendrons. Dendritic blends were miscible up through 12% and exhibited a T_g intermediate between those of the two pure components. With increasing dendrimer content, the free volume of the system increased, as did the molecular mobility of the PMMA chain. This resulted in decreased T_g's for blends up through 12%. Phase separation occurred at and above 15%, as evidenced by Rayleigh scattering in UV–vis spectroscopy data. These data corresponded to the emergence of the phase-separated dendritic glass relaxation (α_D) observed in dielectric measurements. ΔH values, characterized by Arrhenius behavior, were determined for β relaxations before phase separation and were found to slightly decrease with increasing dendrimer content. Glass relaxations in the blends obtained from dielectric experimentation were unable to be characterized by WLF behavior because of the merging of the α and β processes. Electric modulus treatment of dielectric data in the α_D region of the 20% blend resulted in T_g, ΔH, and ΔM values comparable to those found in neat 12-*tert*-butyl ester dendrimer. This confirmed the presence of an isolated dendrimer phase, which coexisted with a partially miscible dendrimer–PMMA phase.

The authors acknowledge Dr. Claus D. Weis of the Center for Molecular Design and Recognition at the

University of South Florida for providing the dendrimer used in this study. They also acknowledge the Division of Sponsored Research at the University of South Florida for the Research and Creative Scholarship Award (J. P. Harmon) and the National Science Foundation (G. R. Newkome; DMR 99-01393), and the Office of Naval Research (G. R. Newkome; N00014-99-1) for their financial support. The authors appreciate Dr. Eleanor Snow for providing the equipment needed for the refractive-index measurements. They also thank Dr. Gregory Baker and Dr. Charles Moorefield for their helpful input.

REFERENCES AND NOTES

1. Archut, A.; Vögtle, F. In Handbook of Nanostructured Materials and Nanotechnology; Nalwa, N. S., Ed.; Academic: New York, 1999; Vol. 5.
2. Bosman, A. W.; Janssen, H. M.; Meijer, E. W. Chem Rev 1999, 99, 1665.
3. Fréchet, J. M. J.; Hawker, C. J. In Comprehensive Polymer Chemistry; Aggarwal, S. L.; Russo, S., Eds.; Elsevier: Oxford, 1996; Suppl. 2.
4. Ihre, H.; Johansson, M.; Malmström, E.; Hult, A. In Advances in Dendritic Macromolecules; Newkome, G. R., Ed., JAI: Greenwich, CT, 1996.
5. Matthews, O. A.; Shipway, A. N.; Stoddart, J. F. Prog Polym Sci 1998, 23, 1.
6. Newkome, G. R.; Moorefield, C. N.; Vögtle, F. Dendritic Molecules: Concepts, Syntheses, Perspectives; VCH: Weinheim, 1996.
7. Tomalia, D. A.; Naylor, A. M.; Goddard, W. A., III. Angew Chem Int Ed Engl 1990, 29, 138.
8. Fréchet, J. M. J.; Hawker, C. J.; Gitsov, I.; Lean, J. W. J Macromol Sci Pure Appl Chem 1996, 33, 1399.
9. Hult, A.; Johansson, M.; Malmström, E. In Advances in Polymer Science: Branched Polymers; Roovers, J., Ed.; Springer-Verlag: Berlin, 1999.
10. Kim, Y. H.; Webster, O. W. In Star and Hyperbranched Polymers; Mishra, M. K.; Kobayashi, S., Eds.; Marcel Dekker: New York, 1999.
11. Malmström, E.; Hult, A. J Macromol Sci Rev Macromol Chem Phys 1997, 37, 555.
12. Newkome, G. R.; Yao, Z.; Baker, G. R.; Gupta, V. K. J Org Chem 1985, 50, 2004.
13. Tomalia, D. A.; Baker, H.; Dewald, J. R.; Hall, M.; Kallos, G.; Martin, S.; Roeck, J.; Ryder, J.; Smith, P. Polym J 1985, 17, 117.
14. Narayanan, V. V.; Newkome, G. R. In Topics in Current Chemistry; Vögtle, F., Ed.; Springer-Verlag: Berlin, 1998.
15. Newkome, G. R.; Moorefield, C. N. In Comprehensive Supramolecular Chemistry; Reinhoudt, D. N., Ed.; Pergamon: New York, 1996.
16. Newkome, G. R. Pure Appl Chem 1998, 70, 2337.
17. Percec, V.; Heck, J.; Johansson, G.; Tomazos, D.; Kawasumi, M.; Chu, P.; Ungar, G. J Macromol Sci Pure Appl Chem 1994, 31, 1719.
18. Zeng, F.; Zimmerman, S. C. Chem Rev 1997, 97, 1681.
19. Hawker, C. J.; Malmström, E. E.; Frank, C. W.; Kampf, J. P. J Am Chem Soc 1997, 119, 9903.
20. Stewart, G. M.; Fox, M. A. Chem Mater 1998, 10, 860.
21. Kim, Y. H.; Webster, O. W. Macromolecules 1992, 25, 5561.
22. Connolly, M.; Ma, B.; Karasz, F. Proceedings of the American Chemical Society Division of Polymeric Materials: Science and Engineering 1993, 69, 82.
23. Massa, D. J.; Shriner, K. A.; Turner, S. R.; Voit, B. I. Macromolecules 1995, 28, 3214.
24. Carr, P. L.; Davies, G. R.; Feast, W. J.; Stainton, N. M.; Ward, I. M. Polymer 1996, 37, 2395.
25. Bauer, B. J.; Topp, A.; Prosa, T. J.; Liu, D.; Jackson, C. J.; Amis, E. J. SPEANTEC 1998, 98, 2065.
26. Bauer, B. J.; Prosa, T. J.; Liu, D.-W.; Jackson, C. L.; Tomalia, D. A.; Amis, E. J. Polym Prepr 1999, 40, 1, 406.
27. Hong, Y.; Cooper-White, J. J.; MacKay, M. E.; Hawker, C. J.; Malmström, E.; Rehnberg, N. J Rheol 1999, 43, 781.
28. Emran, S. K.; Newkome, G. R.; Weis, C. D.; Harmon, J. P. J Polym Sci Part B: Polym Phys 1999, 37, 2025.
29. Young, J. K.; Baker, G. R.; Newkome, G. R. Macromolecules 1994, 27, 3464.
30. Collins, E. A.; Bareš, J.; Billmeyer, F. W., Jr. Experiments in Polymer Science; Wiley: New York, 1973.
31. McCrone, W. C.; McCrone, L. B.; Delly, J. G. Polarized Light Microscopy; McCrone Research Institute: Chicago, 1987.
32. Keyes, D. L. Engineered Materials Handbook; American Society for Metals International: Metals Park, OH, 1988; Vol. 2.
33. TA Instruments DSC 2920 differential scanning calorimeter (TA-087A and TA-230).
34. TA Instruments DEA 2970 dielectric analyzer (TA-057).
35. van Krevelen, D. W.; Hoftyzer, P. J. Properties of Polymers; Elsevier: Amsterdam, 1976.
36. Rao, C. N. R. Ultra-Violet and Visible Spectroscopy Chemical Applications; Plenum: New York, 1967.
37. Harmon, J. P. Polym Prepr 1999, 40(2), 1256.
38. Glen, R. M. Chemtronics 1986, 1, 98.
39. Emslie, C. J Mater Sci 1988, 23, 2281.
40. Harmon, J. P.; Jhaveri, T.; Gaynor, J.; Walker, J.; Chen, Z. J Appl Polym Sci 1992, 44, 1695.
41. Gedde, U. W. Polymer Physics; Chapman & Hall: New York, 1995.
42. Gaynor, J.; Fischer, V.; Walker, J.; Harmon, J. P. Nucl Instrum Methods Phys Res Sect B 1992, 69, 332.
43. Claves, M. C.; Harmon, J. P. In Optical Polymers Fibers and Waveguides; Harmon, J. P.; Noren, G. K., Eds.; ACS Symposium Series 795; American Chemical Society: Washington, DC, 2001.

44. Koenig, J. L. Spectroscopy of Polymers; American Chemical Society: Washington, DC, 1992.
45. Garton, A. Infrared Spectroscopy of Polymer Blends, Composites and Surfaces; Hanser: Munich, 1992.
46. Karasz, F. E. In Polymer Blends and Mixtures; Walsh, D. J.; Higgins, J. S.; Maconnachie, A., Eds.; Martinus Nijhoff: Dordrecht, 1985.
47. Couchman, P. R. Macromolecules 1978, 11, 1156.
48. Fox, T. G. Bull Am Phys Soc 1956, 1, 123.
49. McCrum, N. G.; Read, B. E.; Williams, G. Anelastic and Dielectric Effects in Polymeric Solids; Dover: New York, 1991.
50. Simon, G. P. Dielectric Relaxation Spectroscopy of Thermoplastic Polymers and Blends; Pergamon: Sydney, 1986.
51. Havriliak, S., Jr.; Havriliak, S. J. Dielectric and Mechanical Relaxation in Materials: Analysis, Interpretation, and Application to Polymers; Hanser: Munich, 1997.
52. Dielectric Spectroscopy of Polymeric Materials; Runt, J. P.; Fitzgerald, J. J., Eds.; American Chemical Society: Washington, DC, 1997.
53. Rellick, G. S.; Runt, J. J Polym Sci Part B: Polym Phys 1986, 24, 279.
54. Aihara, T.; Saito, H.; Inoue, T.; Wolff, H.; Stühn, B. Polymer 1998, 39, 129.
55. Bertoluccci, P. R. H.; Harmon, J. P. In Photonic and Optoelectronic; Jenekhe, S.; Wynne, K. J., Eds.; ACS Symposium Series 672; American Chemical Society: Washington, DC, 1995; p 79.
56. Ku, C. C.; Liepins, R. Electrical Properties of Polymers: Chemical Principles; Hanser: Munich, 1987.
57. Aklonis, J.; MacKnight, W.; Shen, M. Introduction to Polymer Viscoelasticity; Wiley Interscience: New York, 1972.
58. Fried, J. R. Polymer Science and Technology; Prentice Hall: Upper Saddle River, NJ, 1995.
59. Catsiff, E.; Tobolsky, A. V. J Colloid Sci 1955, 10, 375.
60. Starkweather, H. W.; Avakian, P. J Polym Sci Part B: Polym Phys 1992, 30, 637.
61. Maxwell, J. C. Electricity and Magnetism; Clarendon: Oxford, 1892; Vol. 1.
62. Wagner, K. W. Arch Electrotech 1914, 2, 371.
63. Sillars, R. W. J Inst Elect Eng 1973, 80, 378.
64. Tsangaris, G. M.; Psarras, G. C.; Kouloumbi, N. J Mater Sci 1998, 33, 2027.
65. Bánhegyi, G.; Hedvig, P.; Petrovic, Z. S.; Karasz, F. E. Polym Plast Technol Eng 1991, 30, 183.
66. van Beek, L. K. H. Progress in Dielectric; Wiley: New York, 1967; Vol. 7.